Case studies of three-dimensional effects on the behaviour of test embankments

Guangfeng Qu, Sean D. Hinchberger, and K.Y. Lo

Abstract: This paper uses both two-dimensional (2D) and three-dimensional (3D) finite element (FE) analyses to examine three cases involving the construction of full-scale test embankments to failure on soft clay deposits. By comparing the calculated fill thickness at failure from 2D and 3D analyses, it is shown that 3D effects are significant for all test fills, despite the dramatically different locations, fill thicknesses, and underlying clay deposits. In addition, the calculated undrained displacement and extent of failure from 3D analysis agree well with those measured in each case. The risk of neglecting 3D effects is highlighted by the analyses, where it is shown that failure to account for 3D effects while interpreting the response of a test embankment can lead to unsatisfactory performance of the actual long embankment. Finally, by comparing FE analysis results with well-known bearing capacity factors, it is shown that test embankments with a base length to width ratio less than 2 are more strongly influenced by 3D effects than spread footings on similar soil profiles. The analyses presented in this paper provide practical insight into some factors that should be taken into account for the design and construction of embankments and test fills on soft clay deposits.

Key words: three-dimensional (3D), geometry effect, embankment, test fill, finite element analysis, case study.

Résumé : Cet article présente trois cas de digues d'essai placées sur des dépôts d'argile molle, de la construction à grande échelle jusqu'à la rupture, qui ont été examinés par analyse d'éléments finis en deux dimensions (2D) et trois dimensions (3D). En comparant les épaisseurs de remblai à la rupture calculées par les analyses 2D et 3D, on observe que les effets 3D sont importants pour tous les remblais testés, malgré les différences considérables dans l'emplacement géographique de chacun des cas, dans l'épaisseur de remblai, et dans les caractéristiques des dépôts argileux sous-jacents. De plus, le déplacement non drainé et l'importance de la rupture calculés à l'aide de l'analyse 3D correspondent bien avec les mesures réelles pour chaque cas. Les différentes analyses mettent en évidence les risques courus lorsque les effets 3D sont négligés. En effet, les analyses ont montré que le fait d'omettre les effets 3D lors de l'interprétation du comportement d'une digue d'essai peut amener à une conception non appropriée de la digue en pleine grandeur. Finalement, la comparaison des résultats de l'analyse par éléments finis avec des facteurs connus de capacité portante permet d'établir que les digues d'essai ayant un ratio de la longueur de la base sur la largeur de moins de 2 sont plus fortement influencées par les effets 3D que lorsque les semelles sont plus étendues, et ce sur un sol de même profil. L'analyse et les résultats présentés dans cet article amènent des connaissances pratiques sur les caractéristiques clés qui devraient être considérées pour la conception et la construction de digues d'essai sur de l'argile molle.

Mots-clés : trois dimensions (3D), effet de la géométrie, digue, remblai d'essai, analyse par éléments finis, étude de cas.

[Traduit par la Rédaction]

Introduction

Trial embankments or test fills are usually constructed to assist in the design of important embankments on difficult foundations (e.g., Dascal et al. 1972; La Rochelle et al. 1974; Tavenas et al. 1974). In some cases, these structures are built to investigate new geotechnical technology such as geosynthetic reinforcement (e.g., Rowe and Soderman 1985; Rowe et al. 1995; Alfaro and Hayashi 1997) or prefabricated wick drains (e.g., Crawford et al. 1992; Bergado et al. 2002). Trial embankments are often heavily instrumented and the foundation soils extensively investigated. As such, these structures make interesting cases for researchers and engineers to study. For most studies involving trial embankments, the geometry is usually simplified to the two-dimensional (2D) plane strain case neglecting the three-dimensional (3D) geometry and its effect (Tavenas et al. 1974; Indraratna et al. 1992; Crawford et al. 1995; Zdravkovic et al. 2002). Thus, it is important to evaluate to what extend 3D effects may influence the collapse height of test fills to improve the interpretation of their behaviour and the performance of the full embankment.

This paper uses the finite element (FE) software ABAQUS, version 6.7.2 (ABAQUS, Inc., Pawtucket, R.I.), to investigate 3D effects on the behavior of three full-scale test fills: the St. Alban test embankment (La Rochelle et al. 1974), the Malaysia trial embankment (MHA 1989*b*; Indraratna et al. 1992), and the Vernon test embankment (Crawford et al. 1995). Back-analysis of these cases highlights some important considerations in the design and interpretation of test embankments. From this study, a shape factor

Received 29 August 2007. Accepted 8 May 2009. Published on the NRC Research Press Web site at cgj.nrc.ca on 10 November 2009.

G. Qu,[1] S.D. Hinchberger, and K.Y. Lo. Geotechnical Research Centre, Department of Civil and Environmental Engineering, The University of Western Ontario, London, ON N6A 5B9, Canada.

[1]Corresponding author (e-mail: guangfengqu@hotmail.com).

Table 1*a*. Parameters for fill materials used in numerical analysis in the three cases.

	Fill materials					
	ϕ' (°)	ψ (°)	c' (kPa)	ν	E (kPa)	γ (kN/m^3)
St. Alban test embankment	44	22	5	0.3	2.0×10^5	19
Malaysia trial embankment	31	15	5	0.3	5.1×10^3	20.5
Vernon case (M profile)	33	16	5	0.3	1.5×10^4	20.5

Table 1*b*. Parameters for soil deposits used in numerical analysis in the three cases.

	Soil layer	Depth (m)	c_{u0} (kPa)	ρ_{cu0} (kPa/m)	γ (kN/m^3)	K_0	E_u (kPa)
St. Alban test embankment[a]	Crust	0–1.6	15	0	19	1.0	1.5×10^4
	Soft clay	1.6–40	7	2.1	17	0.9	2.5×10^4
Malaysia trial embankment[b]	Crust	0–2	25	0	19.8	1.0	2.5×10^4
	Underlying soft clay	2–40	8	1.48	16	0.9	8×10^3
Vernon case (M profile)[c]	Crust	0–6	40	0	20	1.04	1.8×10^4
	Transition layer	6–9	40	–2.67	17	0.85	1.5×10^4
	Soft clay	9–80	32	1.03	17	0.85	2.5×10^4

[a]Plastic index 10%–37% (Trak et al. 1980).
[b]Plastic index 32%–72% (Indraratna et al. 1992).
[c]Plastic index 22%–42% (Crawford et al. 1995).

commonly used in bearing capacity calculations is evaluated for use with 2D embankment collapse calculations.

Methodology

The 2D and 3D behaviour of embankments built on soft cohesive soils was studied using elastoplastic FE analysis. In each case, the embankment fill and foundation soils were discretized using either linear eight-noded brick elements or four-noded plane strain elements for 3D and 2D analyses, respectively. The typical FE mesh comprised a rough rigid boundary situated at the bottom of the soft clayey foundation and smooth rigid boundaries on the lateral sides. Mesh-sensitivity studies were performed to arrive at the final mesh density in each case. The sensitivity studies, which included (*i*) a comparison of calculated and closed-form bearing capacities for rigid footings and (*ii*) a calculation of plane strain collapse heights for embankments using a 2D and 3D thin-slice model, showed that the meshes were capable of giving collapse loads within 5% of the bearing capacity solutions. Some typical meshes are illustrated throughout the paper.

The foundation soils were modeled as isotropic elastic–perfectly plastic materials using the Mohr–Coulomb failure criterion. This constitutive model is commonly adopted in engineering practice due to its simplicity; however, it neglects behavior such as anisotropy, rate-sensitivity, nonlinearity, creep, and strain-softening, which many clays exhibit during loading. For the current study, however, the model is considered to be adequate for comparing the undrained failure of plane strain and 3D embankments constructed quickly on soft clay.

The constitutive parameters for the clayey soils include undrained shear strength (c_u), undrained elastic modulus (E_u), Poisson ratio (ν), bulk unit weight (γ), and coefficient of lateral earth pressure (K_0) defined in terms of the total stresses. A typical undrained shear strength profile comprised a crust underlain by soft clayey soil layers. In all

Fig. 1. Strength profile assumed and measured using field vane and undrained (UU and CIU) tests (experimental data from La Rochelle et al. 1974).

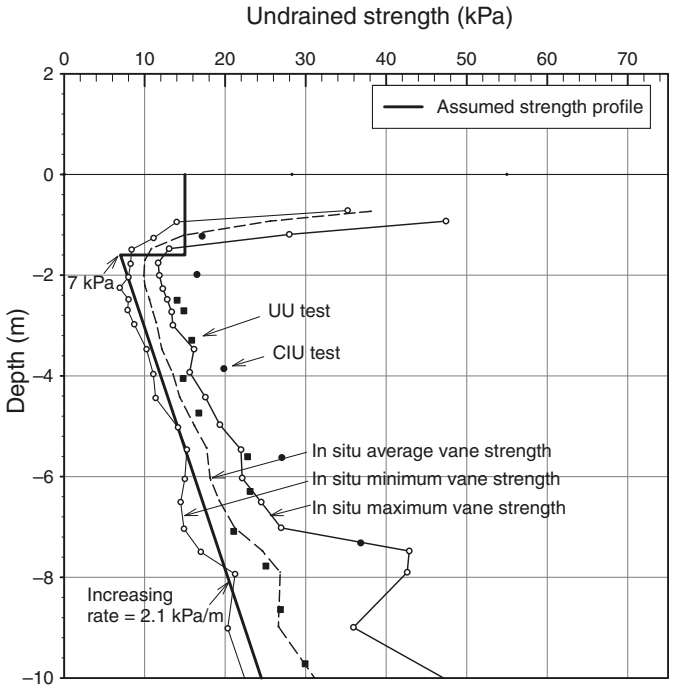

cases, the foundation clay was assumed to have a constant E_u for each layer and failure was assumed to be governed by the Mohr–Coulumb failure criterion with $\phi_u = 0°$, c_u varying with depth, and a dilation angle, ψ, of 0°. Typical foundation layers were idealized as having an undrained shear strength, c_{u0}, at the top of the layer and a gradient of c_u with depth, ρ_{cu0}. The fill was also modeled as an elastoplastic material with a constant Young's modulus (E), Poisson ratio (ν), bulk unit weight (γ), effective friction angle, (ϕ'), cohesion intercept, (c'), and dilation angle (ψ). Soil

Fig. 2. (*a*) Plan view and (*b*) cross section A–A of St. Alban test embankment. All dimensions in metres.

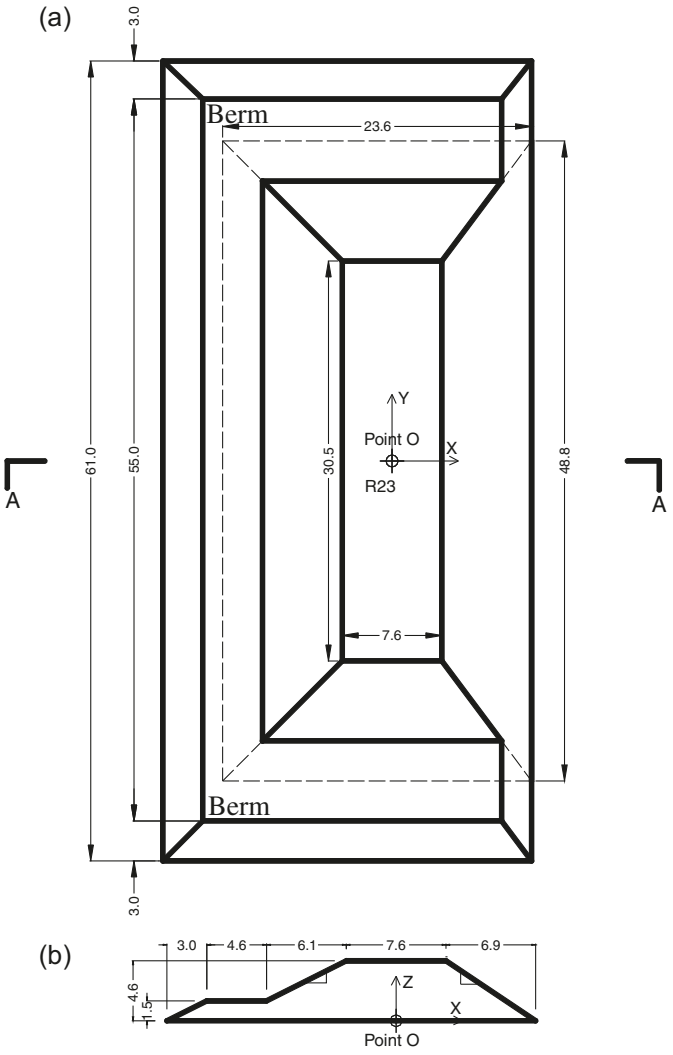

properties for each case are summarized in Table 1 and discussed below.

The construction process was numerically simulated by activating both the weight (body force) and stiffness of fill elements layer by layer using an incremental, iterative, and load-adjusting solution scheme to ensure convergence of the elastoplastic solutions.

St. Alban test embankment case

In 1972, the geotechnical research group of Laval University built four test embankments at Saint Alban, Quebec, to investigate the behavior of embankments on a sensitive Champlain clay. Deposits of Champlain clay are widespread in eastern Canada. In this case, three of the four test embankments were built with different side slopes to study the influence of slope inclination on deformation behavior (La Rochelle et al. 1974) and one of the test embankments was constructed to failure. This latter case was used by Zdravkovic et al. (2002) to demonstrate the effect of strength anisotropy on the embankment behaviour using the 2D MIT-E3 constitutive model (Whittle and Kavvadas 1994), which requires 15 material parameters. In contrast, this paper investigates 3D effects using a simple undrained shear strength profile and elastoplastic analysis.

Fig. 3. Generated meshes for (*a*) 2D and (*b*) 3D finite element method (FEM) models.

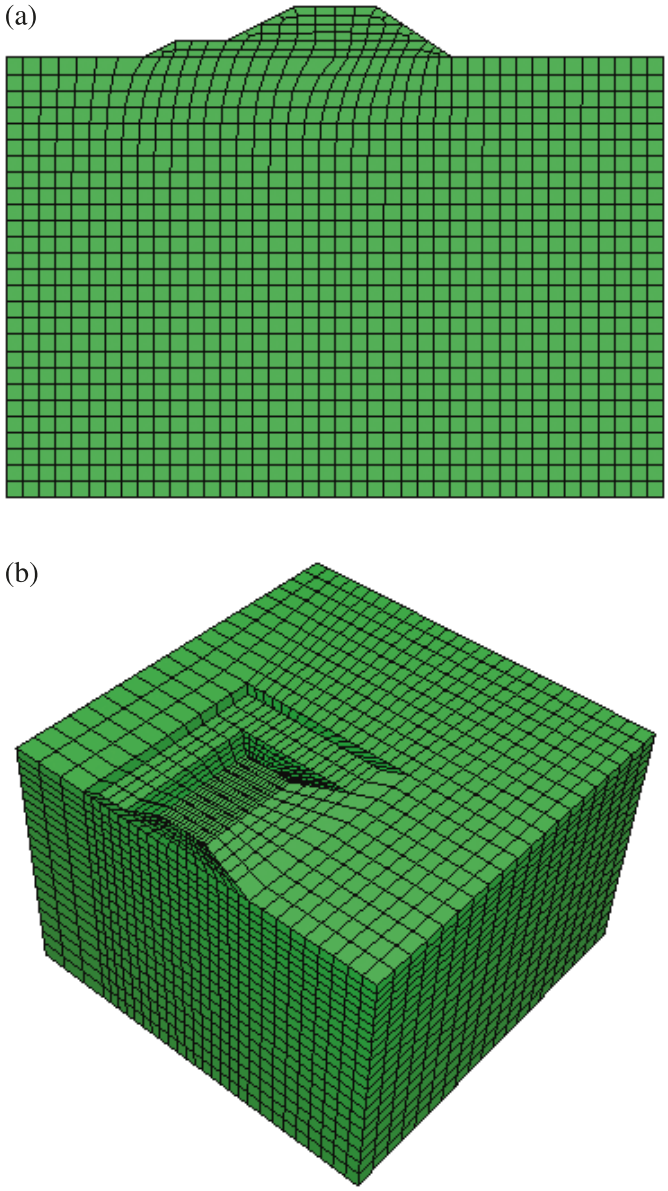

The St. Alban case has also been investigated by Trak et al. (1980), who used 2D limit equilibrium analysis to show that the factor of safety of test embankment "A" at failure (La Rochelle et al. 1974) was 1.20 and 0.93 corresponding to analyses performed using the average vane strength profile and the relationship $c_u = 0.22\sigma'_p$ (where σ'_p is the effective preconsolidation pressure), respectively. From this assessment, Trak et al. (1980) concluded that using $c_u = 0.22\sigma'_p$ for the strength profile was slightly conservative in this case. It is noted that the 3D geometric effect was neglected in the limit equilibrium analysis; whereas, in this paper, 2D and 3D FE analyses are performed to investigate the St. Alban test embankment.

Fig. 4. Measured and calculated vertical displacement of point "O" for St. Alban embankment. $H_{f,2D}$ and $H_{f,3D}$, calculated fill thicknesses at failure for 2D and 3D FE analyses, respectively.

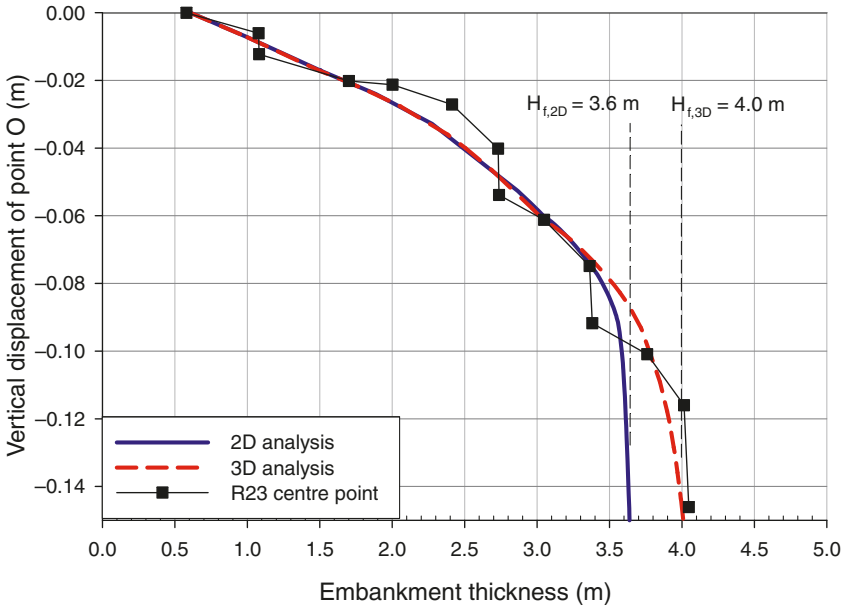

Fig. 5. Spatial displacement contour of 3D model for St. Alban embankment (at failure).

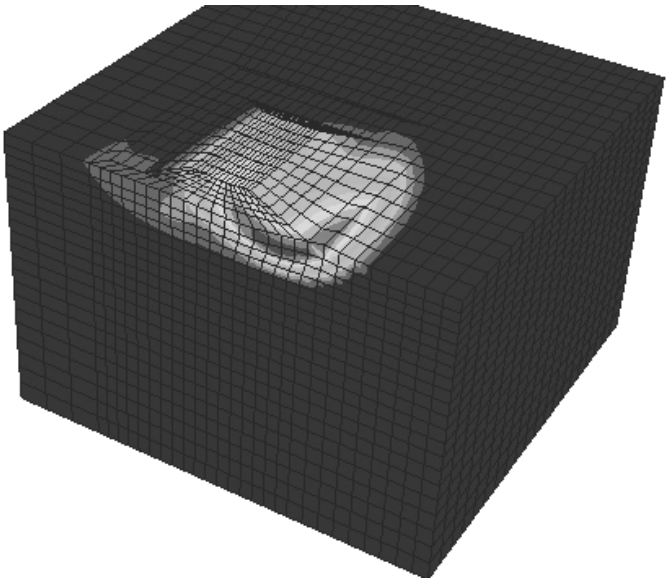

Soil conditions

The foundation at St. Alban comprised a 1.5 m thick weathered crust and a 8 m thick layer of soft silty marine clay, which was underlain by a 4 m thick soft clayey silt. Below the clayey layers was a deposit of fine to medium sand extending to a depth of 24.4 m.

For the analysis of this case, undrained conditions were assumed due to the relatively short period of construction (10 days from 4–13 October 1972) and the low permeability of Champlain clays, which ranges from 10^{-10} to 10^{-9} m/s (Tavenas et al. 1983). As shown by Tavenas et al. (1983), such an assumption is not strictly correct near the drainage boundaries of the clay, but should be adequate to assess the relative behaviour of 2D and 3D embankments.

The Champlain clay deposit has been studied utilizing in situ field vane tests (17 in situ vane tests), cone tests (eight static cone tests), and laboratory tests on tube and block samples (La Rochelle et al. 1974; Tavenas et al. 1974; Leroueil et al. 1979). La Rochelle et al. (1974) noted that in situ field vane and cone tests showed no significant variation of undrained shear strength horizontally across the site, but a relatively typical variation of undrained shear strength with depth. The clay sensitivity varied between 14 and 22; however, the sensitivity was not modeled in the analysis.

Figure 1 shows the measured undrained shear strength from in situ field vane tests and laboratory triaxial tests and the undrained shear strength profile used in the FE analysis of this case (the solid line in Fig. 1). For the FE analysis, the undrained shear strength of the 1.6m thick weathered crust layer was limited to 15 kPa due to the probable existence of fissures in the crust. Below the crust, the undrained shear strength was assumed to increase at a rate of 2.1 kPa/m from 7 kPa at a depth of 1.5m. From Fig. 1, it can be seen that the FE strength profile is close to the lower bound of the field vane tests. As shown in the following section, the assumed profile produces a 3D FE collapse height that is comparable with that actually reported in the case. The assumed undrained elastic modulus and bulk unit weight are summarized in Table 1.

The fill materials consisted of uniform medium to coarse sand with an effective friction angle, ϕ', of 44° based on drained triaxial tests (La Rochelle et al. 1974). For analysis, the dilation angle, ψ, was assumed to be half of the effective friction angle.

Geometry

A plan view and cross section of the test embankment are shown in Fig. 2. The ratio of crest length to width was 4:1 at the designed height of 4.6 m and the corresponding ratio of length to width at the base was about 2:1. The right (front) side slope in Fig. 2*a* was 1.5H:1V and the other

Fig. 6. Spatial displacement contour versus fissures at failure on the top surface of the St. Alban embankment: (*a*) comparison between calculated and observed extents of failure; (*b*) observed failure extent and fissures. ″, inches (1 inch = 25.4 mm).

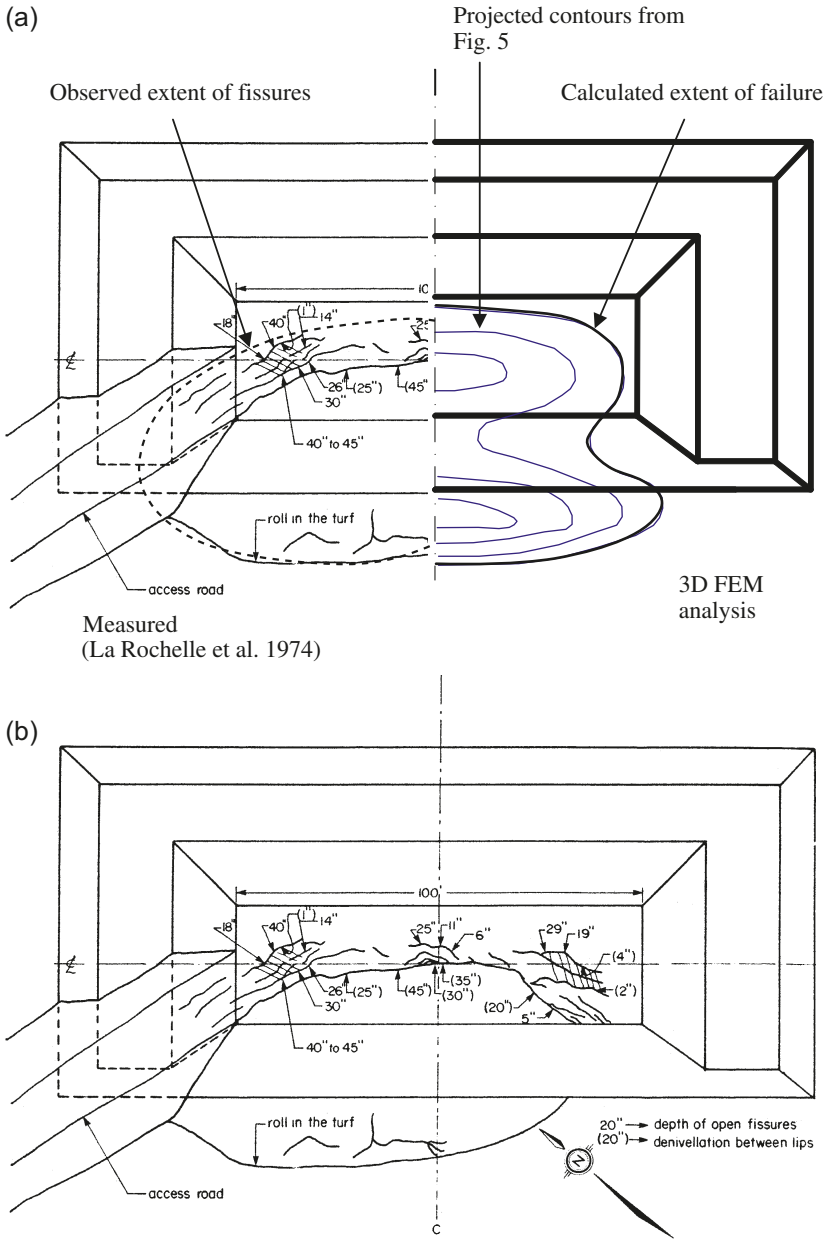

Fig. 7. Statistic table for the prediction of the failure thickness of the Malaysia test embankment (data from MHA 1989*b*).

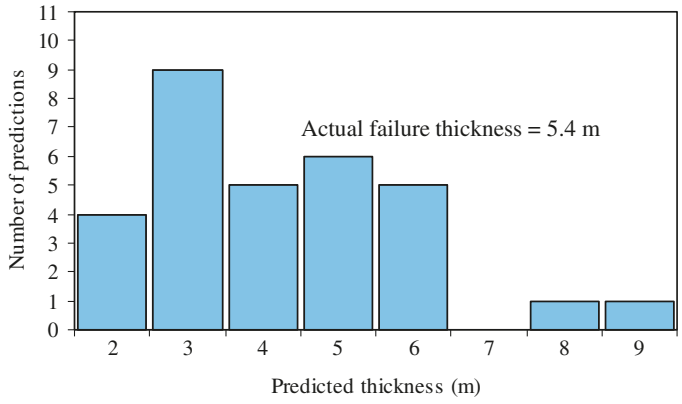

slopes were 2H:1V (where H and V represent horizontal and vertical, respectively). A 1.5 m high berm was placed on the left side and at the ends to ensure the failure occurred on the right side. The test embankment failed at a fill thickness of 4.0 m before reaching the design height.

For analysis, the 2D analysis considered the central cross section A–A as shown in Fig. 2*b*; whereas, the 3D analysis took into account symmetry and thus, only half of the trial embankment was modeled. The 2D and 3D FE meshes are shown in Figs. 3*a* and 3*b* respectively.

Results

As shown in Fig. 4, the calculated fill thicknesses at failure for 2D and 3D FE analyses were 3.6 m and 4.0 m, respectively, based on the vertical displacement curves of the embankment at a central point "O" (see Fig. 2). Despite the 10% difference between predicted failure thicknesses, the magnitude of settlement from both 2D and 3D analyses at the same fill thickness are very similar. Contours of total displacement at failure are shown for the 3D model in Fig. 5, which indicates that the longitudinal extent of the failure mass is restricted by the length of the fill (due to the stabilization effect of both end slopes). In Fig. 6, the observed and computed extents (plan view) of failure are compared, and the agreement is considered to be reasonable. The actual failure mass, however, is slightly rotated relative to that calculated by FE analysis. The rotation appears to have been caused by the access ramp used for construction, which is neglected in the FE calculations. Regardless, it can be seen that the mobilized failure mass for the St. Alban embankment has strong 3D characteristics. As such, failure of the St. Alban test fill is 3D in nature and use of a 2D model results in underestimation of the failure thickness by about 10% compared with that obtained by 3D analysis.

In summary, as expected the 3D FE analysis yields a higher factor of safety than 2D FE analysis for the St. Alban case. In addition, the 3D FE collapse height (4.0 m) is consistent with the collapse height reported in the St. Alban case. This suggests that the mobilized in situ undrained shear strength is similar to the assumed profile depicted by the solid line in Fig. 1. Finally, considering 3D effects, it can be concluded that, had Trak et al. (1980) used 3D limit equilibrium analysis, a factor of safety of about 1.0 would have been obtained, corresponding to an undrained shear strength derived using $c_u = 0.22\sigma'_p$. Such a profile would be comparable to the solid line in Fig. 1.

Malaysia trial embankment case

The Malaysia trial embankment was built to failure at Muar flat in the valley of the Muar River in Malaysia. Muar clay is a very soft clay that caused frequent instability problems during construction of the Malaysian North–South Expressway. The Malaysia trial embankment was built between 27 October 1988 and 4 February 1989. The fill was placed at a rate of about 0.4 m/week until it failed at a fill thickness of 5.4 m.

The Malaysia case was fully instrumented and well documented (MHA 1989*a*). A series of comprehensive field and laboratory tests were carried out before the embankment construction, which provided parameters for researchers and engineers to predict the embankment behavior. An international symposium entitled "Trial Embankment on Malaysian Marine Clays" was held in November 1989 and 31 class "A" predictions of the embankment performance were received from experienced researchers and engineers (MHA 1989*b*), each employing different methods of analysis ranging from stability charts and limit equilibrium analysis to undrained and drained FE analyses (e.g., Brand and Premchitt 1989). In one case, a centrifuge model test was used (Nakase and Takemura 1989). Subsequent to the symposium, Indraratna et al. (1992) reported a calculated failure thickness of 5.0 m using the modified Cam-clay model and 2D FE analysis. All predictions of the failure thickness are summarized in Fig. 7, where it can be seen that there was a wide variation of predicted failure thicknesses ranging from 2.8 to 9.5 m. The majority of predictors underestimated the failure thickness — the average predicted failure thickness was 4.7 m, whereas the actual failure thickness was 5.4 m. This discrepancy reflects the difficulty of geotechnical prediction and also suggests there may be some characteristics that have not been fully explored by the predictors.

Fig. 8. Strength profiles for the Malaysia case (experimental data from MHA 1989*a*).

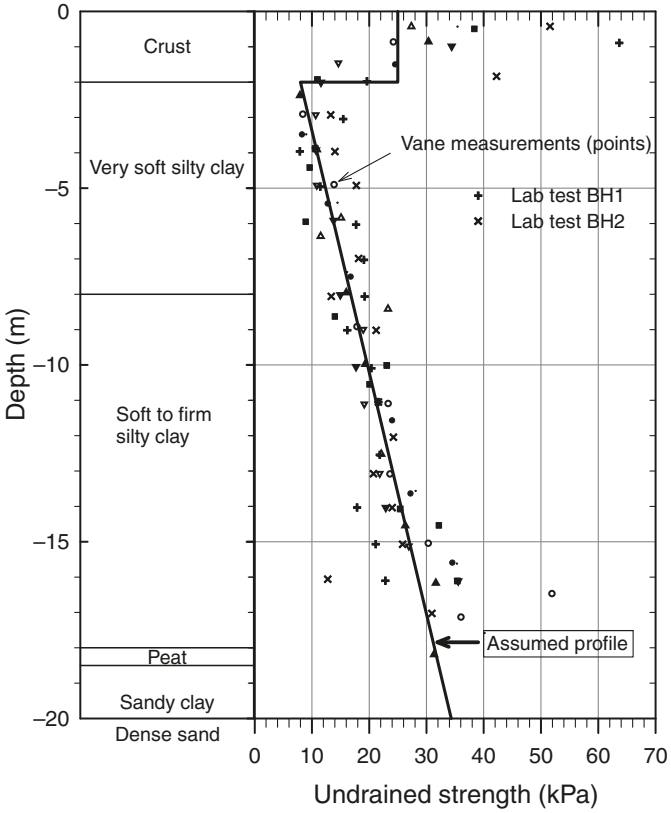

Soil conditions

Figure 8 summarizes the Malaysian soil profile. As reported by the Malaysian Highway Authority (MHA 1989*a*), the subsoil consists of a 2 m thick weathered crust underlain by a 6 m thick deposit of very soft silty clay and a 10 m thick layer of silty clay. The upper clayey deposits overly a 0.5 m peat layer, 3.5 m sandy clay, and then dense sand. According to field and laboratory tests, the undrained shear

Fig. 9. (*a*) Cross section A–A and (*b*) plan view of Malaysia test embankment. All dimensions in metres.

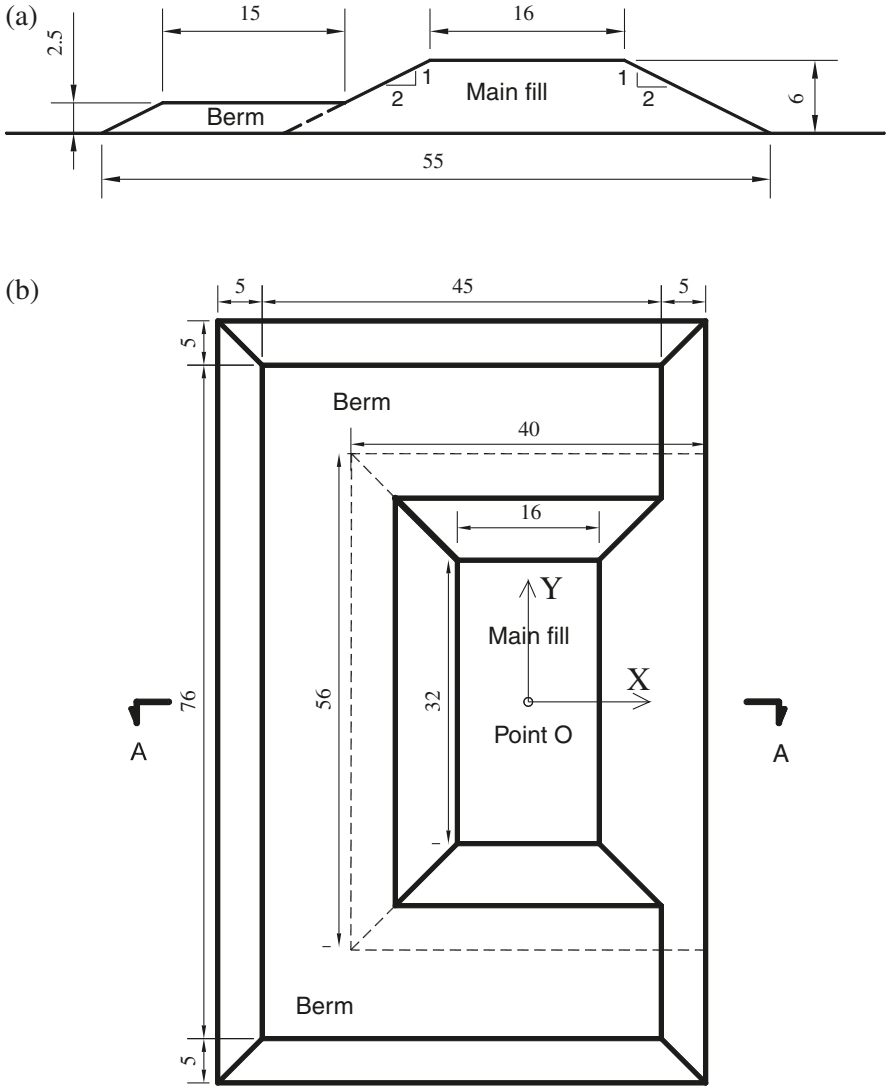

strength increases linearly with depth below the weathered crust.

For FE analysis of the Malaysian case, the clay was idealized as an undrained material even though the time frame for construction was 3 months. As such, this analysis did not take account of partial drainage near the drainage boundaries. The solid line in Fig. 8 depicts the undrained shear strength profile used in the FE analyses. Similar to the St. Alban case, the undrained shear strength of the crust was limited to one-third of the field vane strength to account for the likely presence of fissures (Lo and Hinchberger 2006). All of the engineering parameters of the fill and foundation subsoil used in the FE analyses are summarized in Table 1.

Geometry

A cross section and plan view of the Malaysia trial embankment are presented in Figs. 9*a* and 9*b*, respectively. With respect to the designed thickness of 6 m, the ratio of crest length to width was 2, while the corresponding aspect ratio at the base of the main fill was 1.4. Similar to the St. Alban case, a 2.5 m high berm was placed around three sides of the fill to force the failure toward one side.

Results

Figure 10*a* shows the calculated fill thickness versus vertical displacement at point "O" (see Fig. 9) beneath the center of the embankment. From this figure, it can be seen that the displacement increases linearly as the fill thickness increases during the initial stages of construction. When approaching the failure height, however, a small increase in fill thickness results in large displacement. As shown in Fig. 10*b*, initially the net fill height increases with fill thickness until reaching a maximum value at a critical point, where it decreases with the addition of fill indicating that the incremental vertical displacement exceeds the corresponding increment in fill thickness. When further fill is added, the net fill height decreases and full collapse occurs. Thus, the state with the maximum net height is considered as a critical state and the corresponding thickness is taken as the calculated failure thickness. According to Fig. 10, the calculated failure thicknesses for 2D and 3D analysess are 4.2 and 5.2 m, respectively. Therefore, in the case of the Malaysia test fill, consideration of 3D geometric effects results in a 20% increase in the calculated failure thickness relative to the 2D analysis. In addition, the 3D FE collapse

Fig. 10. (*a*) Measured and (*b*) calculated settlement of Malaysia trial embankment.

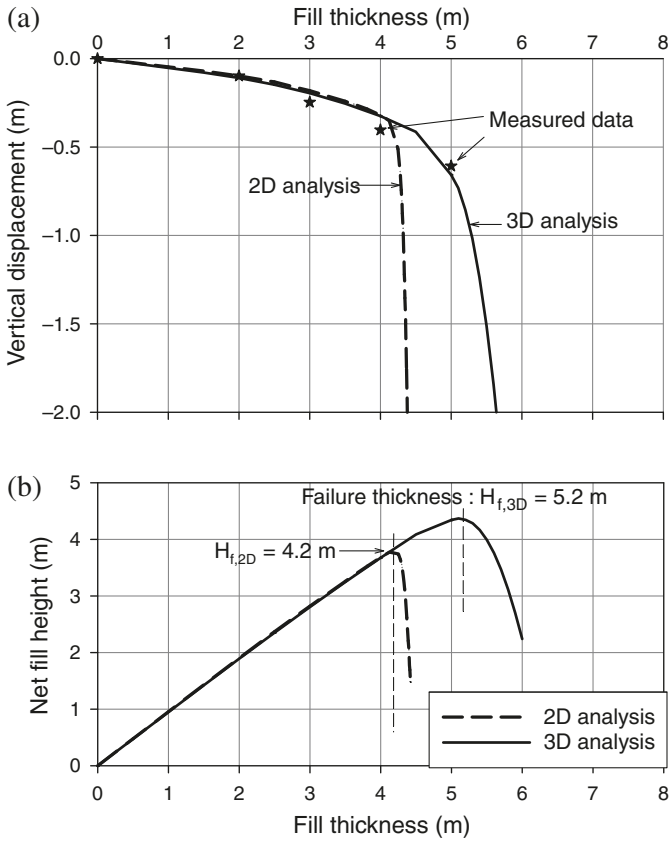

height is within 4% of the collapse height reported in this case.

In Fig. 10*a*, the deformation curve of the 2D model follows closely with that of the 3D model until failure occurs. It appears that in this case the 3D geometry does not significantly influence the deformation prior to imminent collapse. This is consistent with the fact that the calculated settlement by predictors using 2D analysis agreed well with the measured data of the Malaysia trial embankment in spite of the relatively large discrepancy of predicted failure thickness (Brand and Premchitt 1989).

Figures 11 and 12 show the velocity fields at failure for 2D and 3D models, respectively. The trend of movement of the failure mass is shown by the direction of the velocity vectors, and the length of velocity vectors represents the relative magnitude of movement. Both 2D and 3D failure surfaces were estimated based on the velocity fields at the respective failure thickness (4.2 m for 2D analysis and 5.2 m for 3D analysis). As shown in Figs. 11 and 12, the estimated failure surfaces for 2D and 3D analyses are generally comparable although 2D and 3D models predicted different failure thicknesses.

As shown above, the failure thicknesses predicted using 2D and 3D analyses of the Malaysia trial fill differ by about 20%. Thus, neglecting 3D geometric effects will lead to underestimation of the failure thickness. From an engineering point of view, it seems to be conservative to adopt the plane strain assumption. However, to evaluate the strength of the subsoil based on the behaviour of a trial embankment, the 2D model will, in return, lead to an overestimation of the available foundation strength profile, which could lead to inadequate designs for long embankments on such soft soils. This will be discussed and highlighted further during evaluation of the Vernon case below.

Vernon case

The final case considered is the Vernon embankment presented by Crawford et al. (1992, 1995). In this case, two consecutive failures occurred during construction of an approach embankment on soft clay in British Columbia. The embankment failures occurred in spite of the fact that two test fills were built successfully on either side of the failures and that the test fills were higher than the approach embankment that failed.

Figure 13 shows a site plan of the Vernon approach embankment and the location of the two test fills. The Vernon case comprised the West Abutment test fill, which was constructed to a maximum fill thickness of 11.5 m with wick drains in the foundation, and the east test fill or Waterline test fill, which was built to a maximum fill thickness of 12 m without wick drains. Both test fills were constructed in 1986 and remained stable for approximately 3 years before being incorporated into the Vernon approach embankment. Figure 14 shows a cross section of both the Waterline and West Abutment test fills. As the wick drains may have influenced the test fill behaviour, only the Waterline test fill was selected for comparative analysis with the Vernon approach embankment.

Construction of the Vernon approach embankment commenced in early December 1988 and progressed slowly to a fill thickness of between 7 and 9.5 m by 30 June 1989. At this time, the embankment failed (first failure) on the north side encompassing a portion of the West Abutment test fill. The extent of the first failure is shown in Figs. 13 and 14. At the time of the first failure, the West Abutment test fill had been in place for approximately 3 years and according to the results of monitoring, the excess pore pressures generated during construction of this test fill had dissipated (see Fig. 12 of Crawford et al. 1992).

The failed approach embankment was redesigned with 5 m thick and 30 m wide berms on both sides of the original embankment and reconstruction commenced in August 1989 at a very slow rate. In March 1990, a second failure occurred that was much larger in extent and included most of the first failure. The second failure occurred at a fill thickness of about 11.2 m and involved both sides of the approach fill. The extent of the second failure is also shown in Figs. 13 and 14. The approach embankment was eventually completed using berms and lightweight fill; however, the case raises an obvious but perplexing issue: In what way were the results of the two test fills misleading?

Analysis

The subsurface conditions in the Vernon case are summarized in Fig. 15. In the Vernon case, the foundation soils comprised about 4 m of interlayered sand, silt, and clay underlain by a 5 m thick crust comprising stiff to very stiff silty clay, then a deep deposit of soft to firm silty clay (Vernon clay). Figure 15 summarizes the results of field

Fig. 11. Velocity field in central cross section of 2D model for the Malaysia trial embankment (at failure).

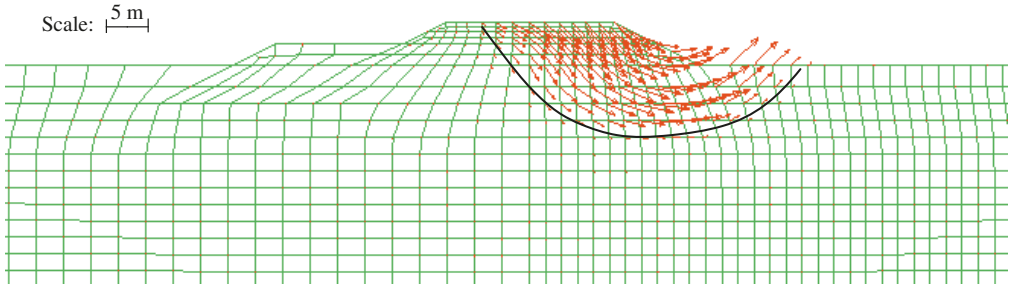

Fig. 12. Velocity field in central cross section of 3D model for the Malaysia trial embankment (at failure). All dimensions in metres.

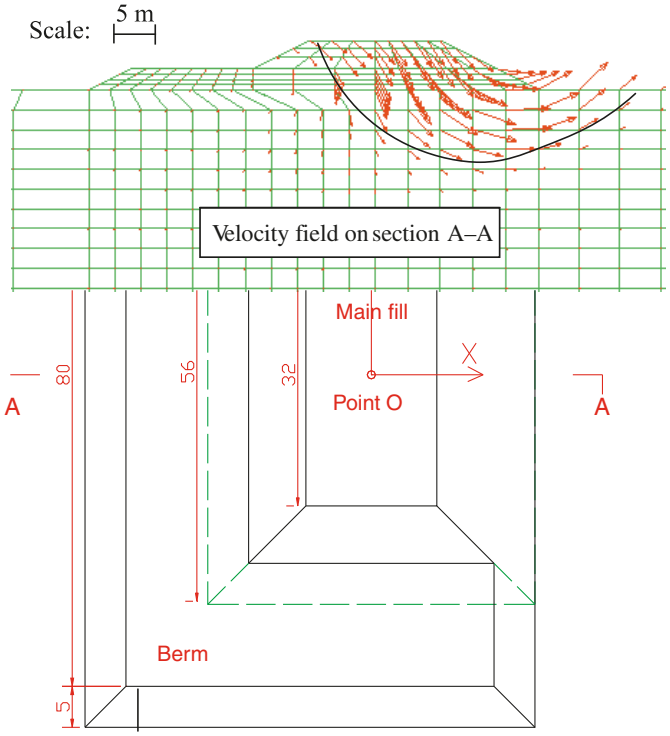

vane tests done in 1960 and 1985 in addition to the undrained shear strength profiles investigated in this study. Unlike the St. Alban case, the sensitivity of Vernon clay varies between 2–4 based on remolded field vane tests, which is relatively low. In addition, Crawford et al. (1995) reported significant variation of undrained shear strength in the upper 8 m of the Vernon deposit corresponding to the crust, and more uniform conditions below 8 m. As such, natural variability in the crust is expected to have had an impact in this case.

For the purpose of analyzing the Vernon case, the undrained shear strength of the crust was limited to 40 kPa in accordance with Lo (1970) and Lo and Hinchberger (2006) to account for the probable effect of fissures on the mass strength of the crust. The undrained shear strength was assumed to be 40 kPa from the ground surface to 6 m deep; it then decreased linearly from 6 m to a depth of 9 m below which the strength increased linearly with depth. Three different strength profiles were investigated: L (0.84M), M, and H (1.08M) that denote lower, middle, and upper strength profiles, respectively (see Fig. 15). The L and H profiles are 84% and 108%, respectively, of the M profile as a whole.

Lo and Hinchberger (2006) studied the 3D effect in this case using 2D plane strain and axisymmetric FE models, where the 3D geometry of the test embankment was simplified as axisymmetric. In addition, the three profiles used by Lo and Hinchberger (2006) have the same crust strength, but a slightly different strength for the soft clay underlying the crust. This paper utilizes a real 3D model to account for the geometry of the test embankments.

Table 1 summarizes the material parameters used in the analysis. The foundation clay was modeled as an undrained material with a unit weight of 16 kN/m^3, friction angle ϕ_u = 0°, and undrained shear strength, c_u, that varied with depth (see Fig. 15). Based on the excess pore pressure response reported by Crawford et al. (1995), the assumption of undrained conditions is considered to be approximately valid. The fill was considered to be a drained material with a unit weight of 20.4 kN/m^3 and effective friction angle, ϕ', of 30°, in accordance with that reported in the case (Crawford et al. 1992, 1995).

The Vernon case was studied using both 2D and 3D FE analyses as described in the following:

(1) The first failure was evaluated using both 2D and 3D FE analyses to obtain an estimate of the mobilized undrained shear strength of the clayey foundation and to investigate the role of 3D effects on the approach embankment performance.

(2) Next, the Waterline test fill was analyzed using 2D and 3D FE analyses.

The back-calculated strength profiles from the 2D (H) and 3D (L) analyses of the Waterline fill are compared with the mobilized strength obtained from the first failure of the Vernon approach embankment. The purpose of these analyses was to investigate the degree to which 3D effects may have affected the performance and consequent lessons learned from the failure of the Vernon approach embankment.

Results of Vernon approach embankment analyses

As shown in Figs. 13 and 14, the Vernon approach embankment was constructed between the Waterline test fill and West Abutment test fill. To evaluate the first failure, station 27+80 was considered for 2D analysis as it is situated at the midpoint of the first failure.

Figure 16 shows the calculated failure thicknesses (8.2 m, 9.8 m, and 10.8 m) corresponding to the L, M, and H strength profiles, respectively. Compared with the actual failure thickness of 9.9 m, the M strength profile provides

Fig. 13. Plan view of Vernon embankment (adapted from Crawford et al. 1995).

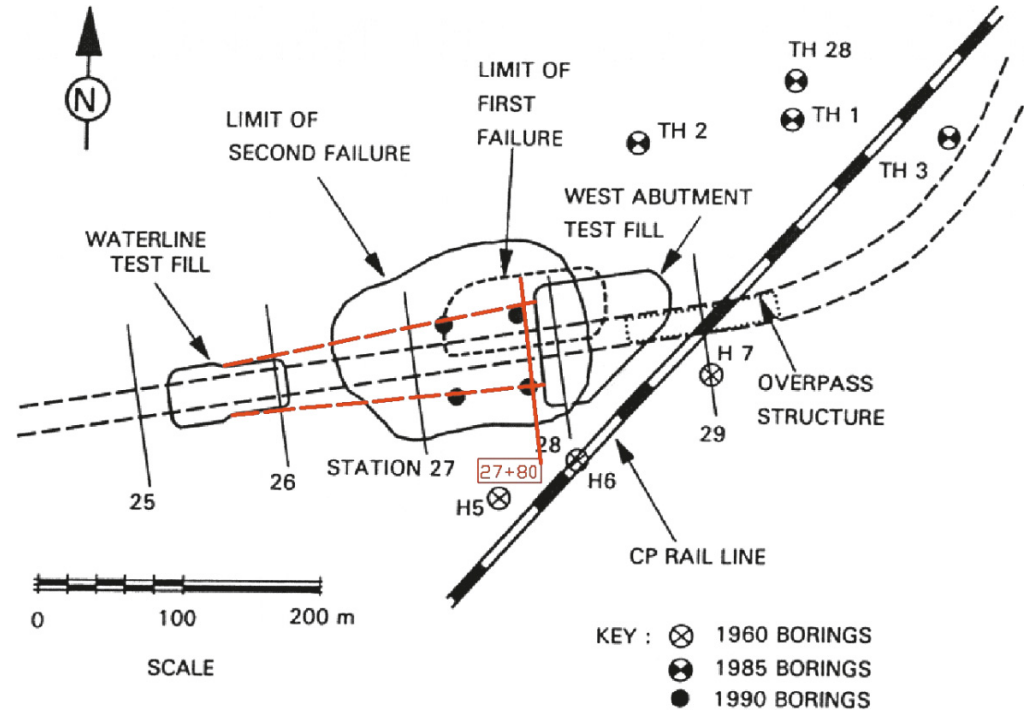

Fig. 14. Longitudinal section through the embankment (after Crawford et al. 1995). SFC., surface.

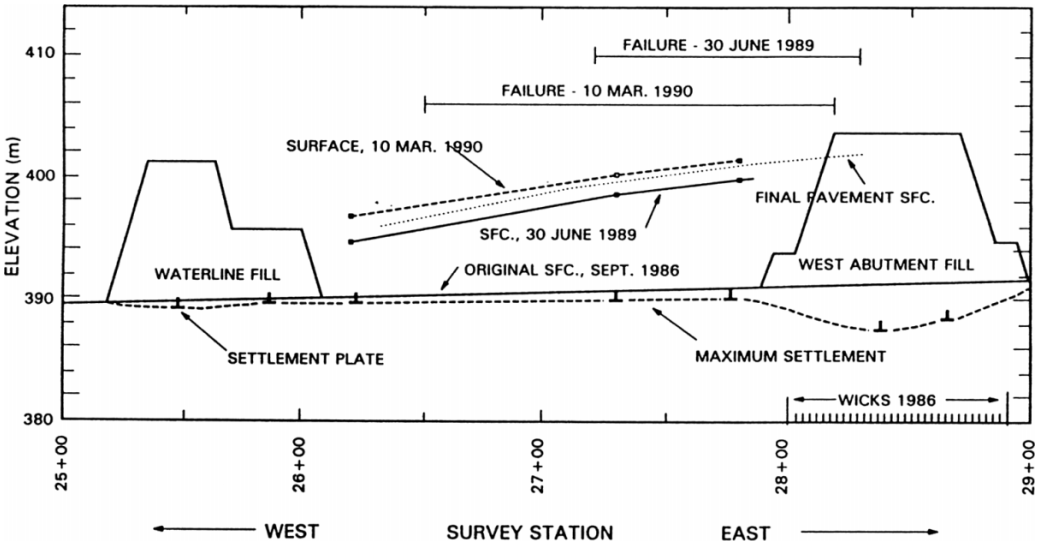

the best fit and is thus considered to be the approximate mobilized strength profile for the first failure from 2D analysis, notwithstanding that there could be other interpretations.

However, the assumed plane strain condition of the first failure may not strictly satisfy the actual condition for the Vernon approach embankment. As shown in Figs. 13 and 17, the height and width of the approach embankment increase toward the bridge site. The longitudinal slope of the embankment crest was also about 3.2% (see Fig. 14). Thus, each cross section in the approach embankment varied geometrically and consequently, the degree of divergence from plane strain condition is unknown.

In light of this, a 3D analysis was done to compare with the 2D analysis discussed above and to explore to what extent the first failure may have been affected by 3D effects. Accordingly, the true 3D geometry of the approach embankment was modelled as shown in Fig. 17. The crest width was constant at 22 m and the side slope gradient was 1.5H:1V. The crest aspect ratio (length/width) was approximately 9.8 and the average base aspect ratio was 4.2. The plan view and cross sections of both ends are shown in Fig. 17.

Figure 18 compares the results of 3D analysis and 2D analysis using the M strengthprofile. The predicted failure thickness from the 3D analysis was 10.3 m, which was 0.4 m higher than the 2D prediction. As the calculated failure thickness of the Vernon approach embankment is only 4% higher for the 3D case compared with that calculated

Fig. 15. Distribution of vane strength with depth.

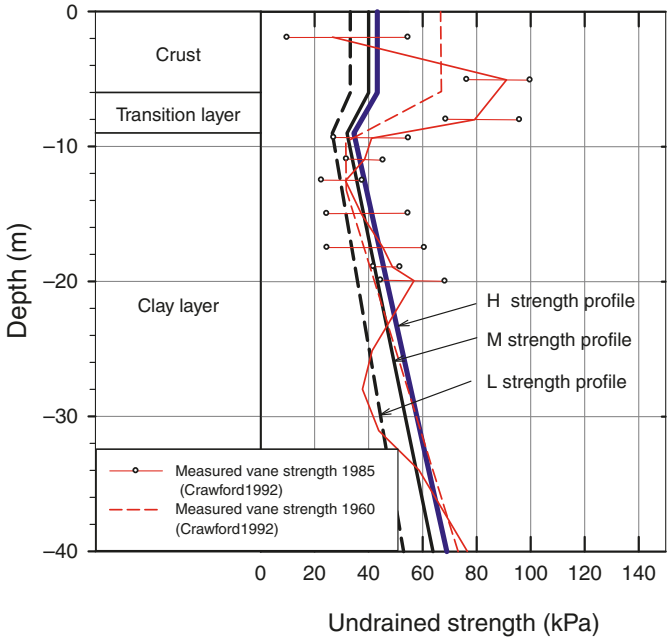

for 2D analysis, it is concluded that the choice of station 27+80 for 2D analysis of the first failure was acceptable.

Figure 19 shows total displacement contours from the 3D model at the failure thickness, together with the vectors indicating the direction and relative magnitude of incremental displacement of the ground surface. The extent of the calculated failure mass is between stations 27+35 and 28+20 and spreads about 50 m outward from the central line. Referring to Figs. 13 and 14, the observed limit of the first failure agrees well with that calculated by the 3D analysis.

Results of Waterline test fill

Because the Waterline fill was used to conclude that the final approach embankment would be stable, the performance of this test fill was analyzed.

For the 2D analysis, the central cross section of the Waterline test fill was considered because of its symmetrical geometry. Figure 20 shows the geometry considered. The measured and calculated displacement of centre point "O" below the Waterline fill are presented in Fig. 21. From Crawford et al. (1995), the measured vertical displacement curve was essentially linear, which indicates that the behaviour of the Waterline fill was predominantly elastic. The predicted fill thicknesses at failure from 2D FE analyses were 8.3 m for the L,10.8 m for the M, and 11.8 m for the H strengthprofiles. Considering that the Waterline test fill was stable at a thickness of 11.8 m, the 2D analysis suggests that the H strength profile represents the lower bound strength available in situ.

A 3D model was undertaken to account for the geometry of the Waterline test fill. The results of the 3D analysis are presented in Fig. 22. From Fig. 22*a*, it can be seen that the calculated failure thickness is 11.8 m using the L strength profile and that the embankment is stable at 11.8 m for both the M and H strength profiles. Thus, it can be deduced from the 3D analysis that the L strength profile is a lower

Fig. 16. (*a*) Net fill height and (*b*) vertical displacement of Vernon approach embankment in 2D analysis.

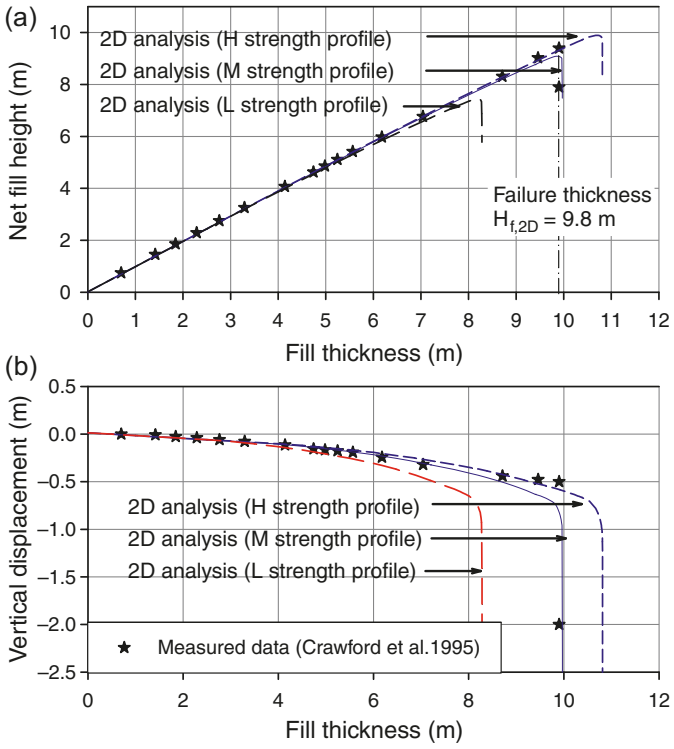

bound for the available in situ foundation strength and that the ratio of 3D to 2D FE collapse thicknesses of the Waterline test fill is 1.4.

Considering the above analyses and discussions, there is a consistent interpretation of the Vernon case. If the M strength profile shown in Fig. 15 is adopted, then a 3D analysis indicates that the Waterline test fill is stable at a fill thickness of 11.8 m, whereas the approach embankment fails at a fill thickness of 9.8 m. This is what was observed in this case. Thus, the 2D and 3D FE analyses suggest that 3D effects may have contributed to the failure of the approach embankment before it reached the height of the adjacent Waterline fill. As noted above, the ratio of 3D to 2D FE collapse thicknesses of the Waterline test fill is 1.4, which is similar to the safety factor commonly used to design such structures, leaving little in reserve for other factors such as soil variability.

Discussion

From the preceding analyses, it has been found that the base aspect ratio (*L*/*B*) of length over width can be utilized to approximately represent the 3D geometry of test embankments. In addition, the ratio of the calculated failure thickness by 3D and 2D FE analyses ($H_{f,3D}/H_{f,2D}$) can be used to quantify 3D effects. $H_{f,3D}/H_{f,2D}$ is plotted against the base aspect ratio (*L*/*B*) in Fig. 23. As shown in Fig. 23, the 3D effect represented by $H_{f,3D}/H_{f,2D}$ is inversely proportional to the base aspect ratio. In addition, the FE data points are qualitatively consistent with the shape factor equation utilized by Skempton (1951) to account for geometric effects on the bearing capacity of spread foundations, e.g.,

Fig. 17. (*a*) Plan view, (*b*) sections, and (*c*) 3D model of Vernon approach embankment. All dimensions in metres.

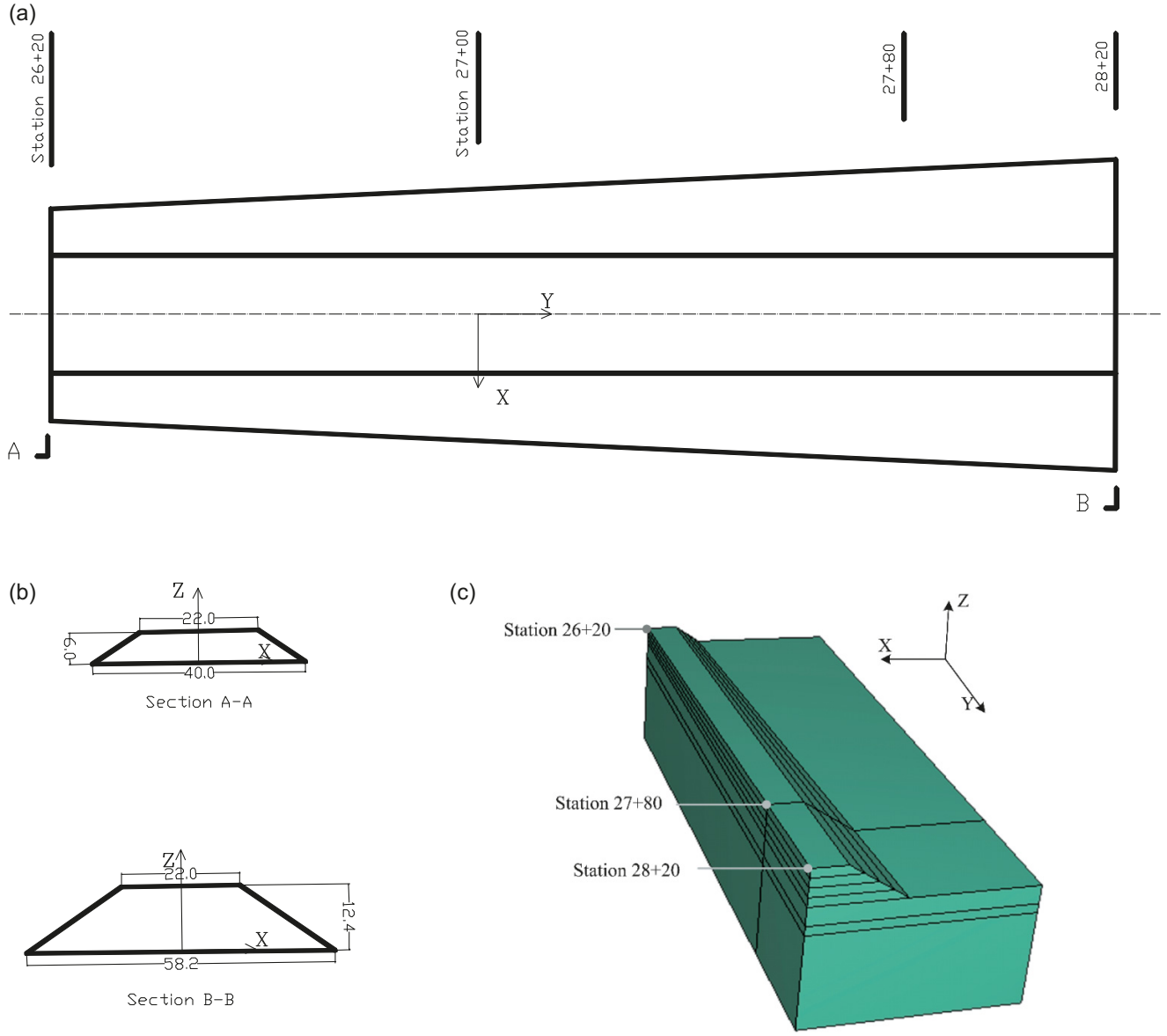

$$[1] \qquad \frac{q_{ult,3D}}{q_{ult,2D}} = 1 + \frac{0.2}{L/B}$$

where L and B are the length and width of the foundation, respectively, and $q_{ult,3D}$ and $q_{ult,2D}$ are the ultimate bearing capacity of a rectangular foundation and the bearing capacity of a infinitely long foundation, respectively.

Equation [1] is plotted in Fig. 23 for comparison with the St. Alban, Malaysia, and Vernon cases. For the Vernon approach embankment and the St. Alban test embankment, the base aspect ratios (L/B) were equal to or larger than 2.0, and the corresponding calculated points in Fig. 23 plot very close to eq. [1]. This suggests that 3D geometry effects on test embankments with an aspect ratio greater than 2 are reasonably close to those deduced from eq. [1]. For the Malaysia trial embankment and the Vernon Waterline test fill, however, the difference between calculated points deviate from eq. [1] by 20% and 40%, respectively, as the aspect ratio decreases from 1.4 to 1.2. The corresponding points representing these two cases in Fig. 23 (from 2D and 3D FE analyses) lie above eq. [1], indicating that 3D effects on test embankments with an aspect ratio less than 2 are greater than that expected for foundation bearing capacity.

In light of the above discussion and comparison, it appears that a simple bearing capacity equation can be used to approximately account for 3D effects on embankments provided the L/B ratio of the base is used. As eq. [1] reflects the relative volume of the failure mass for 3D and 2D geometries, it follows that factors such as the side slope gradient and the presence of berms for the test fills may have influenced the 3D effect to some degree. These factors probably account for some of the difference observed in Fig. 23. However, from an engineering viewpoint, the analyses in this study suggest that a modified eq. [1] corresponding to

Fig. 18. (*a*) Net fill height and (*b*) vertical displacement of Vernon approach embankment in 3D analysis.

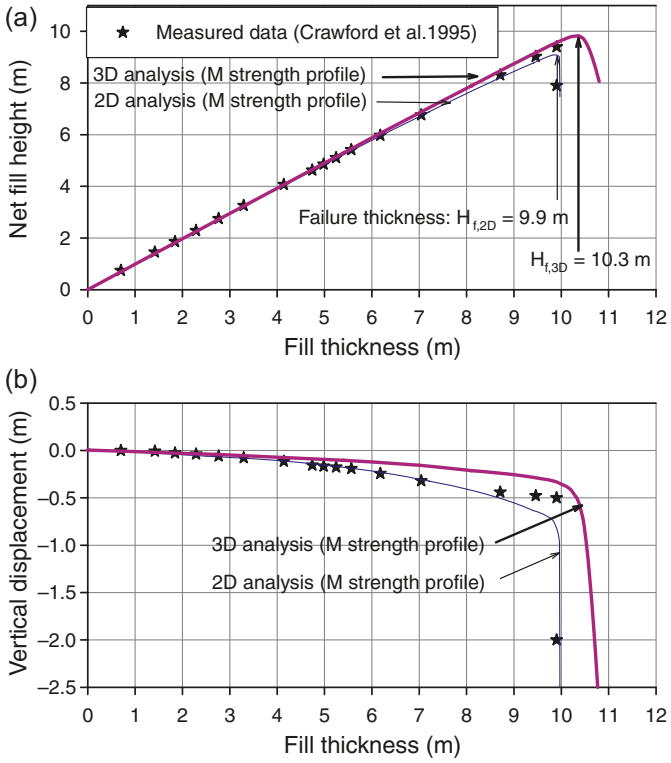

Fig. 19. Spatial displacement contour of Vernon approach embankment.

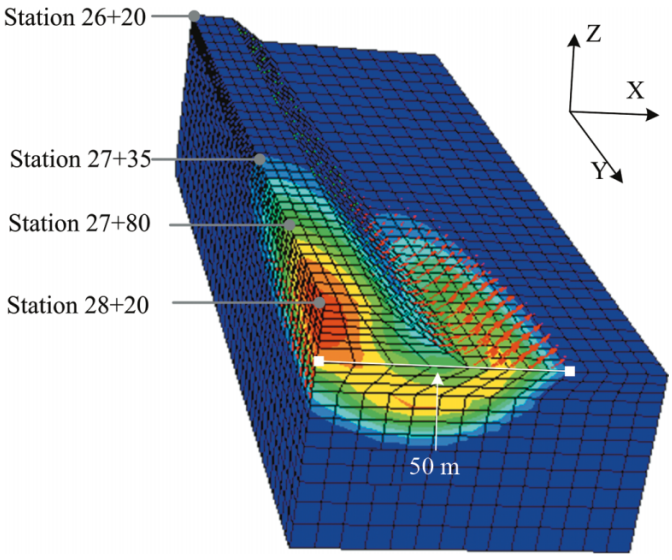

$$[2] \quad \frac{q_{ult,3D}}{q_{ult,2D}} = 1 + \frac{0.3}{L/B}$$

is both simple and potentially adequate for evaluating the 3D effect.

Summary and conclusion

Three full-scale test fills have been evaluated utilizing FE analysis (ABAQUS) accounting for 2D and 3D geometries.

Fig. 20. (a) Plan view and (b) cross section A–A of Waterline test fill. All dimensions in metres.

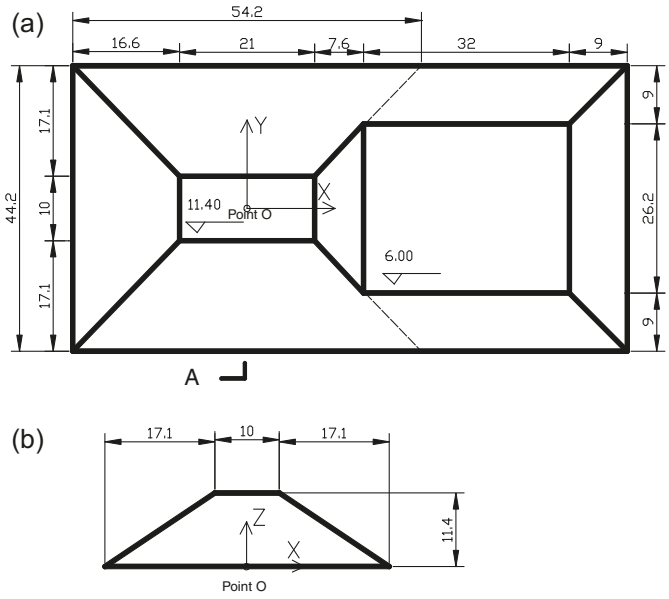

Fig. 21. Measured and calculated (*a*) net fill height and (*b*) vertical displacement by 2D analysis for the Waterline test fill. *H*, fill thickness.

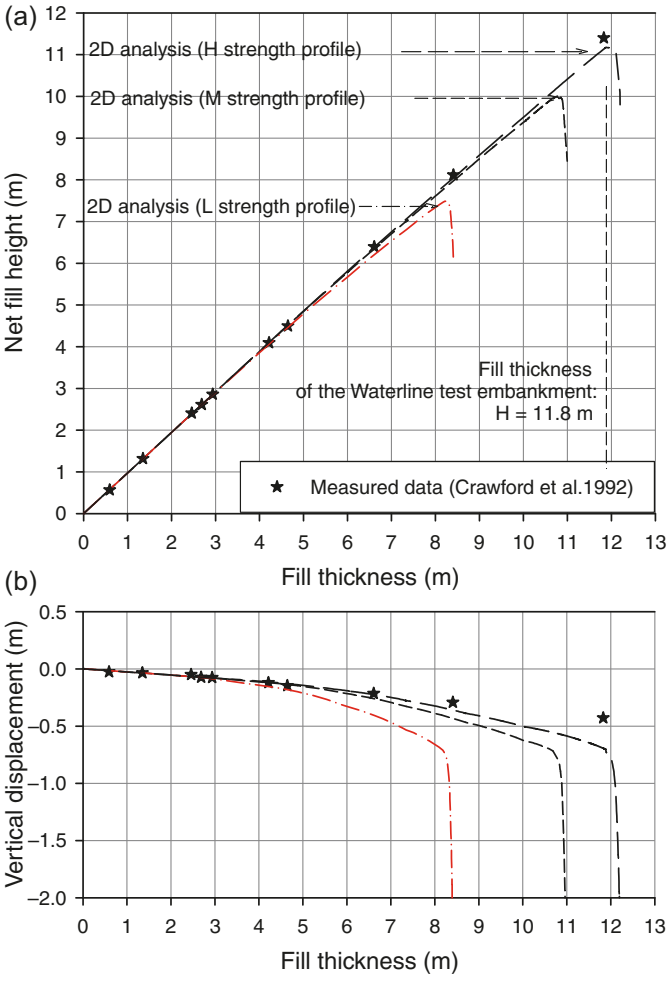

Fig. 22. Measured and calculated (*a*) net fill height and (*b*) vertical displacement by 3D analysis for the Waterline test fill.

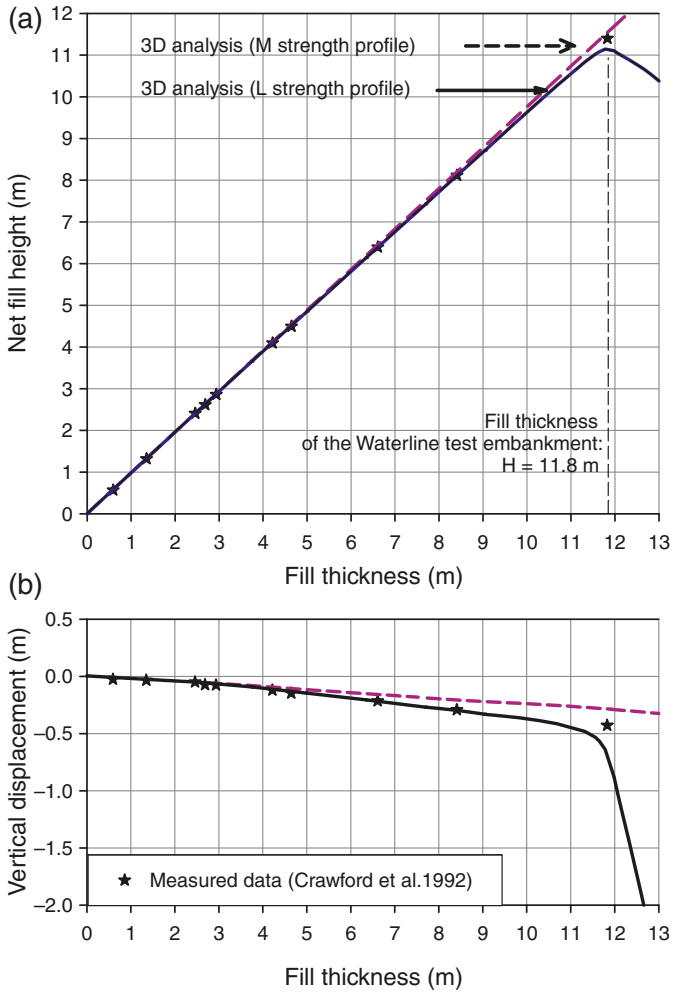

Fig. 23. Illustration of 3D effect on the bearing capacity and the cases studied.

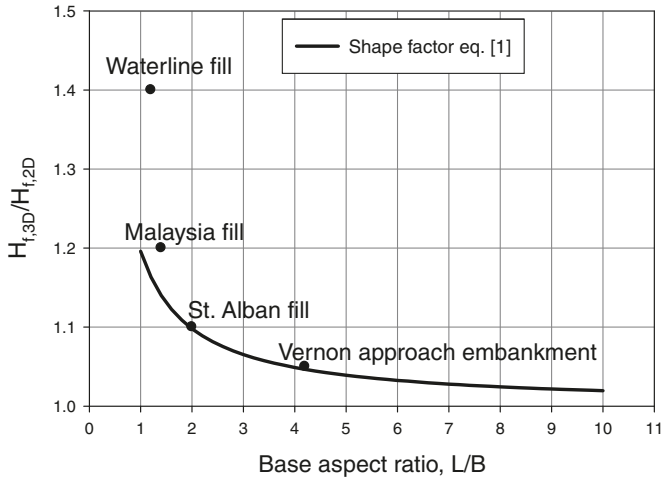

The key findings resulting from these case studies are summarized as follows:

(1) Considerable differences (10% to 40%) of the predicted failure thicknesses obtained by 2D and 3D analyses was found for all three cases. Considering 3D geometry results in an increase in the predicted failure thickness of test fills. This finding is qualitatively consistent with the shape factor equation in bearing capacity theory (Skempton 1951) for base aspect ratios (*L*/*B*) greater than 2. However, when the base aspect ratio is less than 2, the 3D effect on test embankments becomes considerably greater than that suggested by bearing capacity theory.

(2) 3D analysis agrees better with the field behaviour. Beside the influence of 3D geometry, the calculated extent of failure by 3D analysis agrees fairly well with the field observations in the St. Alban and Vernon cases.

(3) Assuming plane strain conditions in the analysis of test fills may potentially lead to the overestimation of the available soil strength and consequently, inadequate design of long embankments on the same site. As shown in the Vernon case, neglecting the 3D geometry and its impact on the behaviour of the Waterline test fill could have been misleading for the design of the long approach embankment.

(4) It is recommended that 3D geometry be considered in the design and interpretation of test fills whose base ratios of length to width are less than 2. In this situation, the influence of 3D geometry should be taken account to reasonably evaluate the behaviour of the trial fills, including the failure thickness, and the mobilized undrained shear strength profiles.

References

Alfaro, M.C., and Hayashi, S. 1997. Deformation of reinforced soil wall-embankment system on soft clay foundation. Soils and Foundations, **37**(4): 33–46.

Bergado, D.T., Fannin, R.J., Holtz, R.D., and Balasubramaniam, A.S. 2002. Prefabricated vertical drains (PVDs) in soft Bangkok clay: A case study of the new Bangkok International Airport project. Canadian Geotechnical Journal, **39**(2): 304–315. doi:10.1139/t01-100.

Brand, E.W., and Premchitt, J. 1989. Comparison of the predicted and observed performance of the Muar test embankment. *In* Proceedings of the International Symposium on Trial Embankments on Malaysian Marine Clay, Kuala Lumpur, Malaysia, 6–8 November 1989. *Edited by* R.R. Hudson, C.T. Toh, and S.F. Chan. Malaysian Highway Authority, Kajang, Selangor, Malaysia. Vol. 2, pp. 10.1–10.29.

Crawford, C.B., Fannin, R.J., deBoer, L.J., and Kern, C.B. 1992. Experiences with prefabricated vertical (wick) drains at Vernon, B.C. Canadian Geotechnical Journal, **29**(1): 67–79. doi:10.1139/t92-008.

Crawford, C.B., Fannin, R.J., and Kern, C.B. 1995. Embankment failures at Vernon, British Columbia. Canadian Geotechnical Journal, **32**(2): 271–284. doi:10.1139/t95-029.

Dascal, O., Tournier, J.P., Tavenas, F., and La Rochelle, P. 1972. Failure of test embankment on sensitive clay. *In* Proceedings of the ASCE Specialty Conference on Performance of Earth and Earth-Supported Structures, West Lafayette, Ind., 11–14 June 1972. American Society of Civil Engineers (ASCE), New York. Vol. 1, pp. 129–158.

Indraratna, B., Balasubramaniam, A.S., and Balachandran, S. 1992. Performance of test embankment constructed to failure on soft marine clay. Journal of Geotechnical Engineering, **118**(1): 12–33. doi:10.1061/(ASCE)0733-9410(1992)118:1(12).

La Rochelle, P., Trak, B., Tavenas, F., and Roy, M. 1974. Failure of a test embankment on a sensitive Champlain clay deposit. Canadian Geotechnical Journal, **11**(1): 142–164. doi:10.1139/t74-009.

Leroueil, S., Tavenas, F., Brucy, F., La Rochelle, P., and Roy, M. 1979. Behavior of destructured natural clays. Journal of the Geotechnical Engineering Division, ASCE, **105**(6): 759–778.

Lo, K.Y. 1970. The operational strength of fissured clays. Géotechnique, **20**(1): 57–74.

Lo, K.Y., and Hinchberger, S.D. 2006. Stability analysis accounting for macroscopic and microscopic structures in clays. *In* Proceedings of the 4th International Conference on Soft Soil Engineering, Vancouver, B.C., 4–6 October 2006. *Edited by* D.H. Chan and K.T. Law. Taylor and Francis, London. pp. 3–34.

MHA. 1989*a*. Factual report on performance of the 13 trial embankments. *In* Proceedings of the International Symposium on Trial Embankments on Malaysian Marine Clay, Kuala Lumpur, Malaysia, 6–8 November 1989. *Edited by* R.R. Hudson, C.T. Toh, and S.F. Chan. Kuala Lumpur. Malaysian Highway Authority, Kajang, Selangor, Malaysia. Vol. 1.

MHA. 1989*b*. The embankment built to failure. *In* Proceedings of the International Symposium on Trial Embankments on Malaysian Marine Clay, Kuala Lumpur, Malaysia, 6–8 November 1989. *Edited by* R.R. Hudson, C.T. Toh, and S.F. Chan. Kuala Lumpur. Malaysian Highway Authority, Kajang, Selangor, Malaysia. Vol. 2, pp. 1-1–1-27

Nakase, A., and Takemura, J. 1989. Prediction of behaviour of trial embankment built to failure. *In* International Symposium on Trial Embankments nn Malaysian Marine Clays, Kuala Lumpur, Malaysia, 6–8 November 1989. *Edited by* R.R. Hudson, C.T. Toh, and S.F. Chan. Kuala Lumpur. Malaysian Highway Authority, Kajang, Selangor, Malaysia. Vol. 2, pp. 3-1–3-13.

Rowe, R.K., and Soderman, K.L. 1985. Approximate method for estimating the stability of geotextile-reinforced embankments. Canadian Geotechnical Journal, **22**(3): 392–398. doi:10.1139/t85-050.

Rowe, R.K., Gnanendran, C.T., Landva, A.O., and Valsangkar, A.J. 1995. Construction and performance of a full-scale geotextile reinforced test embankment, Sackville, New Brunswick. Canadian Geotechnical Journal, **32**(3): 512–534. doi:10.1139/t95-093.

Skempton, A.W. 1951. The bearing capacity of clays. *In* Proceedings of the Building Research Congress, London, 11–20 September 1951. Princes Press, Ltd. Vol. 1, pp. 180–189.

Tavenas, F., Leblond, P., Jean, P., and Leroueil, S. 1983. Permeability of natural soft clays. part I: methods of laboratory measurement. Canadian Geotechnical Journal, **20**(4): 629–644. doi:10.1139/t83-072.

Tavenas, F.A., Chapeau, C., La Rochelle, P., and Roy, M. 1974. Immediate settlements of three test embankments on champlain clay. Canadian Geotechnical Journal, **11**(1): 109–141. doi:10.1139/t74-008.

Trak, B., La Rochelle, P., Tavenas, F., Leroueil, S., and Roy, M. 1980. New approach to the stability analysis of embankments on sensitive clays. Canadian Geotechnical Journal, **17**(4): 526–544. doi:10.1139/t80-061.

Whittle, A.J., and Kavvadas, M.J. 1994. Formulation of MIT-E3 constitutive model for overconsolidated clays. Journal of Geotechnical Engineering, **120**(1): 173–198. doi:10.1061/(ASCE)0733-9410(1994)120:1(173).

Zdravkovic, L., Potts, D.M., and Hight, D.W. 2002. The effect of strength anisotropy on the behaviour of embankments on soft ground. Géotechnique, **52**(6): 447–457. doi:10.1680/geot.52.6.447.38738.